

# Longitudinal AC Breakdown Voltage of XLPE-XLPE Interfaces Considering Surface Roughness and Pressure

Emre Kantar, Frank Mauseth, Erling Ildstad

Department of Electric Power Engineering  
Norwegian University of Science and Technology  
Trondheim, 7491, Norway

and Sverre Hvidsten

Department of Electric Power Technology  
SINTEF Energy Research  
Trondheim, 7465, Norway

## ABSTRACT

The interfacial breakdown between two dielectric surfaces has been reported to represent one of the principal causes of failure for power cable joints and connectors; thus, a better understanding of interfacial breakdown mechanisms is vital. The primary purpose of this paper is to investigate the influence of the surface roughness and interfacial pressure on the tangential AC breakdown strength (BDS) of solid-solid interfaces experimentally. The three-dimensional surface texture parameters are utilized to characterize the morphology of the surfaces. Experiments were performed using samples made of cross-linked polyethylene (XLPE) at three different contact pressures. The surface roughness was varied by polishing the surfaces using four different sandpapers of different roughness. Each surface topography was then assessed using a 3-D optical profilometer. Next, the samples were assembled under ambient laboratory conditions. The experimental results showed a good correlation between the tangential BDS and the surface roughness. The results suggested that reducing the surface roughness resulted in decreased mean height of the surface asperities by nearly 97% and increased the real contact area of the interface considerably. As a result, the tangential BDS rose by a factor of 1.85 – 2.15 with increasing pressure. Likewise, the increased contact pressure yielded augmented tangential BDS values by a factor of 1.4 – 1.7 following the decrease of the roughness.

Index Terms — Breakdown, cable connector, cable joint, dielectric, interface, interfacial pressure, surface breakdown, surface roughness, tracking failure, XLPE.

## 1. INTRODUCTION

CABLE connectors are vital components of oil and gas installations and future offshore renewable energy systems. Although materials and production technologies for power cables have gained a fair amount of experience over the years, cable connectors and joints, where solid-solid interfaces emerge, are still considered the weaker parts of complete cable systems [1, 2]. The combination of two solid dielectrics adversely affects the dielectric performance due to the increased risk of interfacial tracking failure, leading to the formation of a conductive path bridging the electrodes [1–7].

One of the main reasons of solid interfaces being weaker than the bulk solid material is caused by the inhomogeneous electric field distribution at the interface since interfaces mostly arise between different materials with different relative permittivity [2, 5]. Besides, interfaces are generally mated during assembly at the site in sub-optimal and less controllable conditions, which renders them rather vulnerable to bad installations [2]. As a consequence, microscopic imperfections (such as cavities, protrusions, and contaminants) occur at the interfaces. Such

imperfections reduce the AC electric breakdown strength (BDS) of the interface notably, particularly when the electric field has a tangential component since the tangential component traverses the interface [1, 2, 5]. Even in the cases when the magnitude of electric field is much lower than the dielectric strength of the bulk insulation, the imperfections at the interface cause local electric field enhancements due to the difference in permittivity. They are, thus, likely to initiate partial discharges (PD), electrical treeing and a complete flashover might eventually follow [3, 4, 6].

Study of insulating materials and BDS of applications for cables and accessories have been covered to a large extent in the literature [1–10]. The impact of contact pressure and surface roughness on the tangential BDS have been covered in [1, 2, 5, 6, 10], and it has been reported that higher interfacial pressure and smoother surface led to an increased BDS. There is, however, still a lack of knowledge on the dominating mechanisms in the interfacial breakdown phenomenon, while the majority of research articles focus on the complete designs of joints and accessories as a whole. This holistic approach makes the problem even more complicated once the simpler causes of failures are disregarded to allow more complex phenomena to be examined [1]. Nor is there sufficient experience on the performance of interfaces under electrical

and mechanical stress [2]. Besides, growing demands of the industry to provide higher power at higher service voltages stipulate significant and cost-effective developments to the cable joints and accessories [3]. In short, the interfaces are inevitable and bring the highest degree of uncertainty; hence, studying their role is of paramount importance.

The primary purpose of this paper is to explore the impact of the surface roughness and mechanically applied interfacial pressure on the longitudinal AC breakdown strength of dry-mated polymer interfaces experimentally. The 3-D areal field parameters are also utilized when differentiating the morphology of the surfaces quantitatively to help interpret the experimental findings. The polymer interfaces in cable splices, joints, and connectors are usually comprised of a soft and a hard material (i.e. XLPE-EPDM, XLPE-SiR, XLPE-EPR), or between two identical polymers, such as XLPE-XLPE. A soft material will provide a better contact and sealing even under low/moderate pressures [1, 2]. The methodical approach adopted in this work favors the XLPE-XLPE interface as the polymer interface since the key purpose is to examine an interface where the materials involved have the same elasticity and can withstand high pressures without any significant deformation over a broad pressure range.

## 2.BACKGROUND

### 2.1 MORPHOLOGY OF THE DIELECTRIC SURFACES

The assembly of interfaces does not follow an automated process under clean room conditions, nor is any factory inspection done before commissioning. Thus, a cavity-free interfacial surface is not possible to obtain [2]. The protrusions on a dielectric surface vary in size and distribution as shown in Figure 1. When two dielectric surfaces come to contact, plenty of cavities are formed between the tips of the interfacial protrusions. As a result, the contact spots take up far less space than the cavities as can be envisaged from Figure 1 (also from the surface topography in Section 4.1). A typical cavity formed at the interface is elongated in the tangential direction ( $y$ -axis) as illustrated in Figure 2.

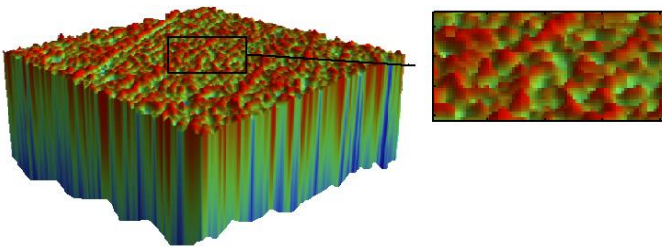


**Figure 1.** An example of a 3-D texture of interfacial surfaces encountered in dielectric interfaces.

When the interface is assembled under dry conditions, the cavities are filled with air. The applied voltage is then distributed along the strings of the cavities and contact spots. Since the dielectric strength of air is much lower than that of the polymer insulation, the dielectric breakdown will first occur in the air-filled cavities, and then the complete flashover presumably takes place immediately [1, 3]. In the case of a homogeneous electric field, the correlation between the cavity

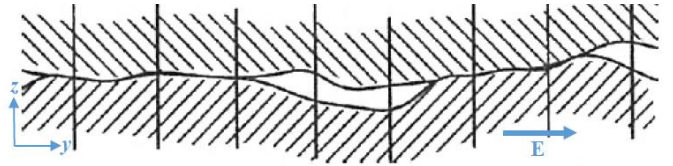


**Figure 2.** An illustration of the expected channel-shaped cavity in two-dimensional profile subjected to the tangential electric field.

size and the breakdown voltage (BDV) is characterized by the Paschen's curve for air [11]. Referring to the left side of the Paschen's curve for air (the left branch of the  $v$ -shaped curve), Majid et al [4] addressed that as the cavity length increases, the expected BDV thereof reduces. Considering the findings of Majid et al [4] and the inspection of the surfaces after dielectric breakdown in Section 4.1, we infer that there are a number of air-filled channels spreading out across the entire interface. Channels are considered a series of cavities linked as a string at the interface in 3-D plane, they are, thus, vented to the surroundings, and the pressure inside them remains at atmospheric pressure. Besides, the vented channels coexist with numerous interlocked smaller cavities in which the air pressure is likely to increase as the contact pressure is increased. The BDV of vented channels is, however, much lower than that of the individual interlocked cavities according to Paschen's law [4]. Therefore, vented channels are assumed to be the principal governing mechanism in the interfacial breakdown phenomenon.

### 2.2 CORRELATION BETWEEN THE SURFACE TEXTURE AND THE BREAKDOWN STRENGTH

A comprehensive approach modeling the electrical breakdown phenomenon between two dielectric surfaces is far-fetched since the number of the parameters involved varies significantly depending on the test environment and the test set-up itself. In addition to this stochasticity, the exact length and number of the channels and cavities are unknown and depend heavily on the following parameters: *the elasticity of the material, the applied interfacial pressure, and the surface roughness*. The correlation between the interfacial BDS and each of these parameters has been studied to a large extent in the literature. As illustrated in Figure 3, when the electric field traverses the interface tangentially, the increased contact

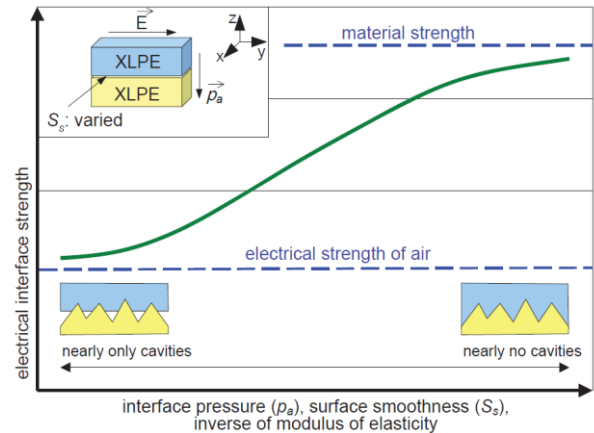


**Figure 3.** The tangential breakdown strength of the interfaces against the interface pressure and the surface roughness/smoothness ( $S_s$ ).

pressure (i.e. interface pressure) renders the interfacial BDS higher [5]. The reason for this is the increased pressure further pushes the tips of the protrusions and renders the cavities smaller that in turn augment the interfacial BDS. The impact of the pressure on the cavity structure is illustrated in Figure 4 on a two-dimensional surface texture profile obtained from a virgin XLPE sample polished by #500-grit sandpaper. (Details of the procedure are provided in Section 3.) There, two surfaces, one rough and one nominally flat (zero-axis) are assembled, and the rough surface is pushed towards the flat surface. As seen, the floating asperities come to contact with the flat surface, and the area of contact expands as the pressure is augmented from 0.5 MPa to 2.2 MPa. The yielded maximum cavity size; thus, shrinks from 129  $\mu\text{m}$  to 25  $\mu\text{m}$ . These results were obtained by employing the *deterministic approach* in [12] that makes use of the obtained surface texture profiles and computes the displacement of the peaks and pits with respect to the applied contact pressure and material properties [12]. However, it is beyond the scope of this work, and Figure 4 is used to reveal the effect of the contact pressure quantitatively.

Likewise, smoother surfaces show as similar an influence on the BDS as the increased pressure, due to the reduced cavity size at the interface. It is worth mentioning that the interfacial BDS is higher than that of air, whereas it is not as strong as the bulk material strength even under a higher contact pressure or a smoother surface [5]. The impact of the surface roughness and the interfacial pressure on the BDS will be interpreted in the discussion using the correlations and premises provided here.

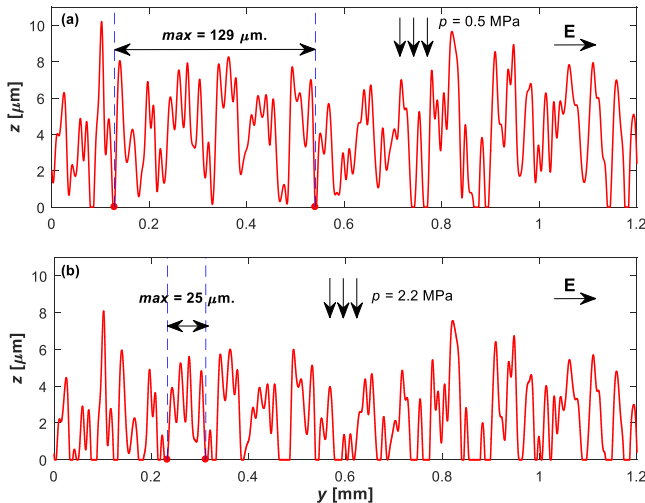


**Figure 4.** The displacement of peaks and dips on the measured surface profile under the contact pressure of: (a) 0.5 MPa. (b) 2.2 MPa.

### 3. EXPERIMENTAL PROCEDURE

#### 3.1 THE SET-UP FOR AC BREAKDOWN TESTS

A simple illustration of the test arrangement with the dimensions of the core components is depicted in Figure 5. There, two rectangular prism-shaped samples (55 mm x 4 mm x 25 mm) were placed on top of each other under dry ambient conditions between two Rogowski-type electrodes, forming a 4 mm-wide interface traversed by the tangentially applied electric field. A detailed sketch of the mechanical test set-up is shown in Figure 6. The two brass electrodes hold the specimens

together with the aid of a helical compression spring (no. 4), which pushes one electrode (no. 3) towards the other. In this way, the distance between the electrodes is restricted to the width of the specimens. The desired contact pressure was exerted using weights ranging between 11 – 26 kg (no. 5) on the weight-carrying plate (no. 6) to press the samples towards one another vertically (z-axis). All breakdown tests were performed with the set-up immersed in transformer oil to prevent any external flashover. To avoid oil migration to the interface, we applied the load before filling the test chamber with the oil. This procedure is referred to as “dry-mated interfaces”.

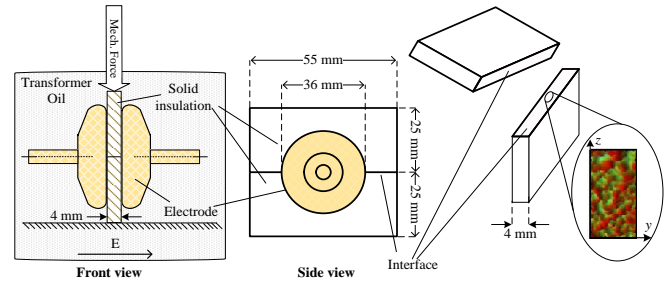


**Figure 5.** The simplified sketch of the mechanical test set-up.

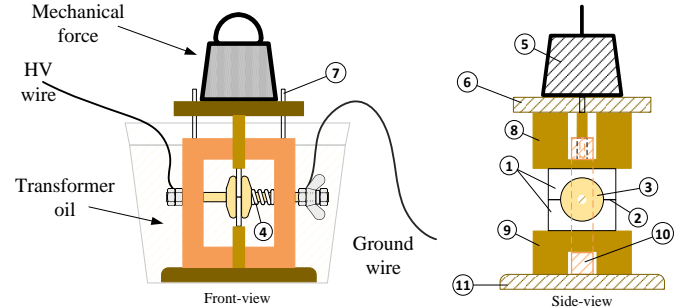


**Figure 6.** Detailed sketch of the mechanical test set-up: (1) Specimens. (2) Polymer interface. (3) Rogowski electrodes. (4) Helical spring. (5) Weight. (6) Weight-carrying plate. (7) Slender weight stabilizer rods. (8) Movable (upper) interface pressure transfer block. (9) Fixed (lower) interface pressure keeper block. (10) Supporting frame structure. (11) Base wooden plate.

A variac (0 – 230 V, 50 Hz) was used to energize the primary side of a 100 kV transformer, generating an AC ramp voltage on the secondary winding at the rate of 1 kV/s. A water resistor was employed to limit the breakdown current as shown in Figure 7. Also, a voltage divider was employed to measure the applied voltage. The voltage was recorded using a data acquisition unit connected to a PC.

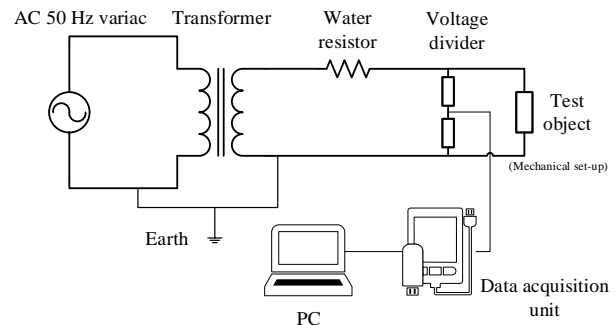


**Figure 7.** The sketch of the overall electrical test set-up.

### 3.2 PREPARATION OF THE SAMPLE AND SURFACE

XLPE samples were cut in the size of 55 mm x 4 mm x 25 mm rectangular prisms from the insulation of a commercially available 145 kV power cable. The contact surfaces of the samples were prepared using *STRUERS Abramfin* microprocessor controlled, tabletop, rotating grinding machine. As shown in Figure 8, the specimens were fixed on a steel rotating disk, and a round-SiC sandpaper of the desired grit was placed on the rotating plane. Four different sandpapers of different grits (#180, #500, #1000, and #2400) were used. The speed of the rotating plane was set to 150 rpm, and the force that presses the steel disk towards sandpaper was fixed to 3 MPa during polishing of all the samples, making sure that the surfaces were subjected to the same grinding procedure.

The samples were sanded for 2–3 minutes with a continuous flow of water to remove any by-products and residues, and to avoid heating caused by friction. Subsequently, the samples were rinsed in tap water and were left to dry. Then, the dry samples were cleaned using filtered compressed air before they were washed briefly in isopropanol. Finally, they were dried at room temperature.



Figure 8. Surface preparation of the aligned and fixed specimens.

### 3.3 EXAMINATION OF THE SURFACE TOPOGRAPHY USING A 3-D OPTICAL PROFILOMETER

A 3-D optical profilometer (*Bruker Contour GT-K 3-D Optical Microscope*) was used to obtain the surface topography of the polished XLPE surfaces. The assessment area of the profile was 1.26 mm x 0.95 mm, which was about 5.5% of the total interface area  $A$  (4 mm x 55 mm). Several scans were performed at different sections on each surface to ensure consistency.

The three-dimensional areal surface roughness  $S$ -height parameters are evaluated according to ASME B46.2-1995 standard and are shown in Figure 9 in a two-dimensional profile [13]. They are namely:

- arithmetic mean height/roughness ( $S_a$ ),
- RMS height/roughness ( $S_q$ ),
- the maximum profile peak height ( $S_p$ ),
- the minimum profile peak height ( $S_v$ ), and
- the maximum height of the surface ( $S_z$ ).

As Leech [13] and Jones et al [14] suggested, the  $S_a$  and  $S_q$  parameters represent an overall measure of the surface texture, and they can be used to identify the different surfaces under study, where  $S_q$  is typically used to specify optical surfaces, and  $S_a$  is used for machined surfaces. Thus,  $S_a$  will be utilized in the first place when a brief comparison is exercised.

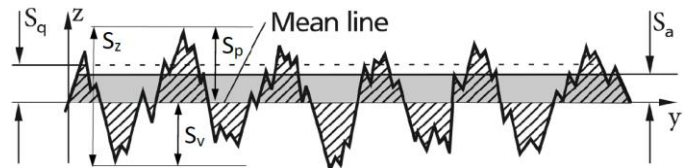


Figure 9. The schematic representation of the  $S$ -parameters.

### 3.4 TEST PROCEDURE & DATA PROCESSING

Initially, BD tests were performed to identify the minimum and maximum pressure levels that the constructed set-up permits without oil ingress and significant deformation of the samples. We determined the minimum pressure as 0.5 MPa—achieved by using weights amounting to 11 kg—below which we had detected partial oil-ingress. Likewise, the maximum pressure was limited to 1.16 MPa—by weights adding up to 26 kg—because no significant improvement in the tangential BDS was observed above that level.

Dry-mated XLPE-XLPE tests for each rough surface were conducted at 0.5, 0.86, and 1.16 MPa average contact pressure  $p_a$ . Each contact pressure is roughly calculated using  $p_a = F/A$ , where  $F$  is the exerted force in N. For each set of experiments, eight BDV measurements were performed using a virgin pair of samples, i.e. a virgin sample is used only once.

The obtained results were statistically evaluated using the two-parameter Weibull distribution. The adequacy of each Weibull curve was checked using the goodness of the fit waveform provided in [15]. For further evaluation, the 63.2 percentile value with its 90% confidence interval was used.

In case of no breakdown at the interface, the corresponding measurement was not disregarded; but was considered as a censored value and was treated accordingly, following the recommendations in [15]. As a result, two types of data emerged, namely complete data and singly censored data [15]. Only complete data will be depicted in the figures; whereas, censored data will be mentioned when necessary.

## 4. RESULTS

### 4.1 SURFACE CHARACTERIZATION

The 3-D surface topographies of all the surfaces polished by #180, #500, #1000, and #2400 grit sandpapers are shown in Figure 10. The polished surface in Figure 10a appears to be quite rough with an irregular pattern of spikes composed of high peaks and deep pits/valleys; whereas, it becomes far less irregular with shorter peaks and shallower pits from Figure 10b to 10d. The obtained roughness  $S$ -height parameters from the measurements are tabulated in Table 1.

Using the profilometer, we also obtained the surface height of a quarter of the interface width of the roughest and the smoothest surfaces in the  $yz$ -plane, respectively (see Figure 11). The units of  $y$ - and  $z$ -axes reveal that the formed cavities are much larger in the  $y$ -direction as illustrated in Figure 2. Also, the breakdown path caused by the alleged vented channels at the surface of the broken-down samples of #180 and #2400 at 0.86 MPa are demonstrated in Figure 12. In the case of #180, the channel is 926  $\mu\text{m}$ -wide whereas it is as narrow as 17  $\mu\text{m}$  in the case of #2400.

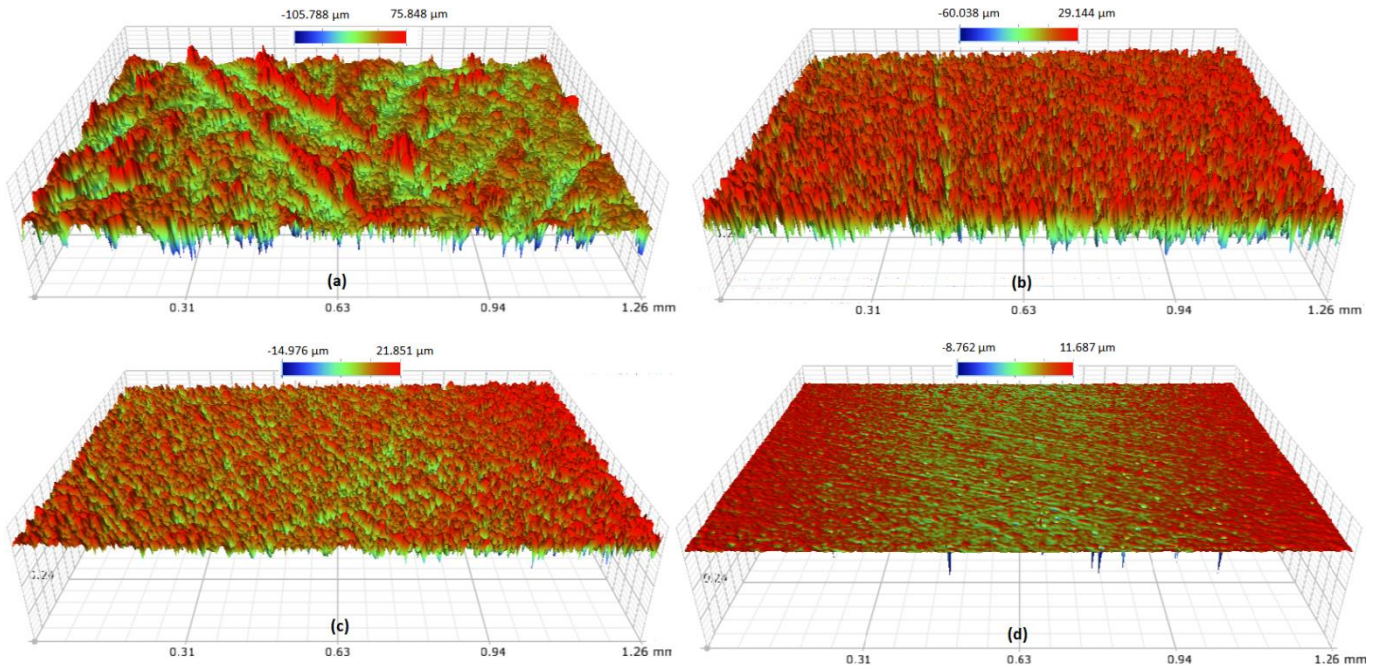


**Figure 10.** 3-D surface inspection of interfacial dry surfaces of the sample ground by the sandpaper grit: (a) #180. (b) #500. (c) #1000. (d) #2400.

**Table 1.** Surface roughness height parameters.

Grit no.	Roughness $S$ -parameters [ $\mu\text{m}$ ]				
	$S_a$	$S_q$	$S_p$	$S_v$	$S_z$
#180	8.86	12.50	75.85	-105.79	181.64
#500	7.79	9.57	29.14	-60.04	89.18
#1000	1.65	2.19	21.88	-14.98	36.86
#2400	0.27	0.60	11.69	-8.76	20.44

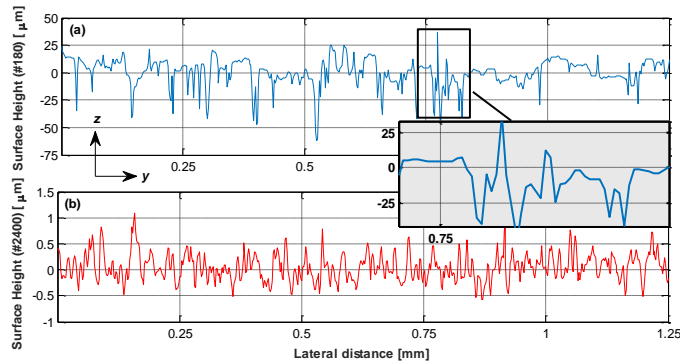


**Figure 11.** The measured surface topography of XLPE sampled ground using: (a) #180-grit sandpaper. (b) #2400-grit sandpaper.

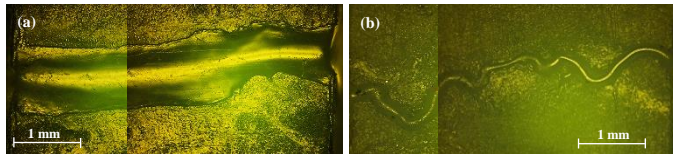


**Figure 12.** The breakdown channels of the samples tested at 0.86 MPa: (a) #180 (channel width: 926  $\mu\text{m}$ ). (b) #2400 (channel width: 17  $\mu\text{m}$ ).

#### 4.2 AC BREAKDOWN TESTS

Figures 13, 14, and 15 display the influence of the surface roughness on the interfacial BDS under 0.5, 0.86, and 1.16 MPa contact pressures, respectively. They also feature the 90%

confidence interval of the 63.2 percentile value for each case. The results show that, in each case, an increased roughness (i.e. higher  $S_a$ ) results in a reduced BDS, not to mention an increased contact pressure brings about an increased BDS as evident in Figures 13–15.

Only the 63.2 percentile values are plotted against the sandpaper grit in Figure 16 to facilitate the interpretation whereas each bar graph illustrates the arithmetic mean height  $S_a$ . The 63.2 percentile BDS in the case of an interface ground by #2400 is nearly twice as high as that of the interface ground by #180 under each pressure. The improvement in the 63.2 percentile BDS from #180 to #500 and from #180 to #1000 is; however, not as notable, only by a factor of 1.2 – 1.3. Finally yet importantly, Figure 17 demonstrates the impact of the interfacial pressure for each rough surface in a separate plot. Referring to Figures 16 and 17 and interpreting the effect of the pressure and roughness together, we can infer that the 63.2 percentile BDS becomes 1.4 times as high for  $S_a = 8.86 \mu\text{m}$  (#180). Whereas, it increases by a factor of 1.7 for  $S_a = 0.27 \mu\text{m}$  (#2400) as the pressure is raised from 0.5 to 1.16 MPa.

## 5. DISCUSSION AND FURTHER INVESTIGATION

The primary purpose of this section is to interpret the experimental BDS results along with the performed surface inspection and to discuss the validity of the assumptions made in Section 2.

The rate of change in the 63.2 percentile BDS from #1000 to #2400 culminates under each pressure as can be seen in Figure 16, where the highest improvement is seen at 1.16 MPa by a factor of 1.6. Thus, it can be inferred that the smoothness of the surface can play as vital a role as the interfacial pressure in improving the BDS of the polymer interfaces under dry-mated conditions.

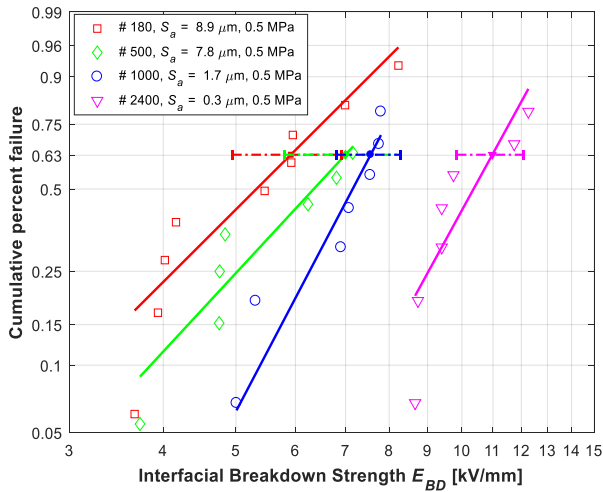


**Figure 13.** The Weibull plot showing the cumulative percent failure regarding the BDS of dry the XLPE-XLPE interface at 0.5 MPa.

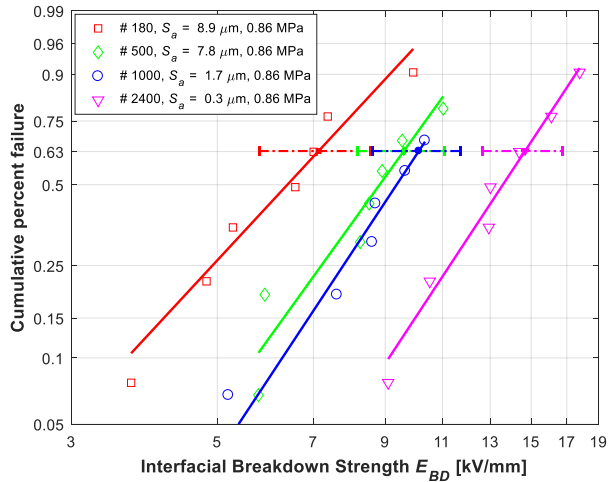


**Figure 14.** The Weibull plot showing the cumulative percent failure regarding the BDS of dry the XLPE-XLPE interface at 0.86 MPa.

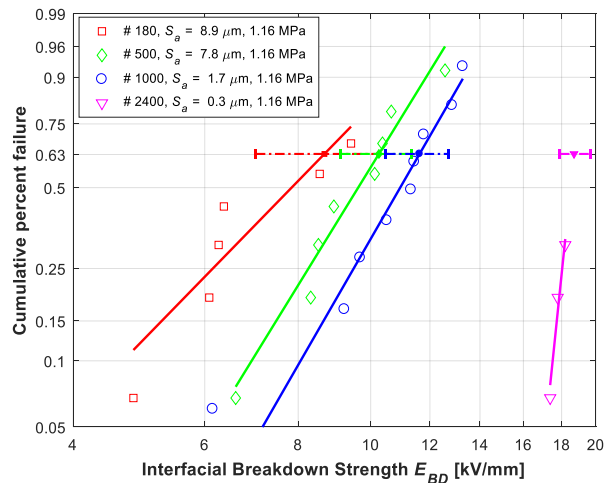


**Figure 15.** The Weibull plot showing the cumulative percent failure regarding the BDS of dry the XLPE-XLPE interface at 1.16 MPa.

In Figure 17, as  $S_a$  reduces by a factor of 32 from #180 to #2400, the 63.2 percentile BDS increases by 85% at  $p_a = 0.5$  MPa. Similarly, it rises by 115% at 1.16 MPa. Interpreting the

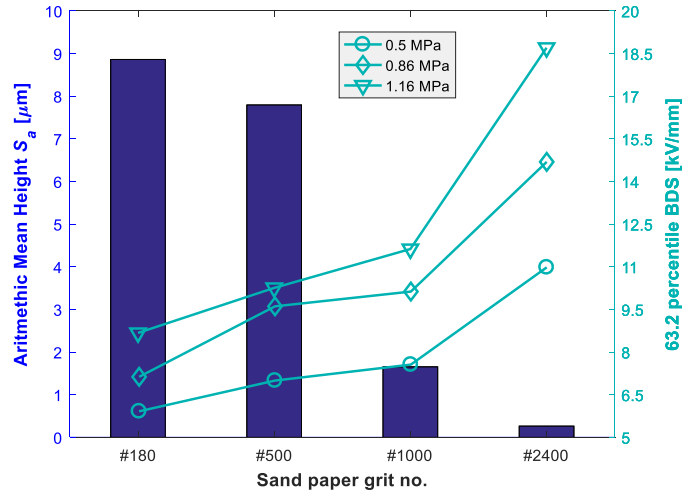


**Figure 16.** (i) Left y-axis: Arithmetic mean height  $S_a$  shown by bar graphs. (ii) Right y-axis: The 63.2 percentile BDS versus the sandpaper grit no.

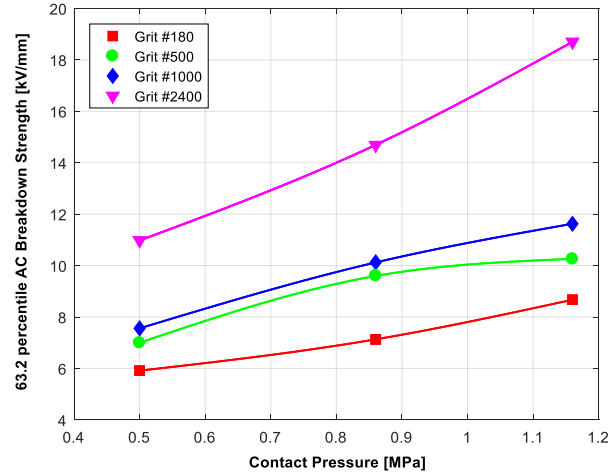


**Figure 17.** The 63.2 percentile AC breakdown strength versus applied contact pressure.

impact of the pressure regarding the correlation introduced in Section 2.2, we deduce that increased interfacial pressure probably reduces the size of the air-filled cavities at the considered surface, where the biggest change in BDS by a factor of 1.7 was observed in the case of the smoothest surface. The significant difference in the surface height between the surfaces in Figure 11 is quite likely to cause a substantial deviation in the size of the cavities in the  $yz$ -plane, where the smoother surfaces yield much thinner cavities in the vertical direction. Such cavities, narrow in the vertical axis and wide in the horizontal direction as depicted in Figures 2 and 11, undergo the lowest stress factor (i.e. unity) as addressed in [16]. The stress factor stands for the ratio of the enhanced field inside the cavity to that of outside the cavity (in the insulation) under a uniform electric field [16]. Consequently, the lower the stress factor, the higher the interfacial BDS.

$S$ -hybrid parameters; namely, the number of summits per unit area ( $S_{ds}$ ), mean summit curvature ( $S_{sc}$ ), and developed interfacial area ratio ( $S_{dr}$ ) are also employed to compare the 3-D surface texture quantitatively (see Table 2). It was interesting to have observed the  $S$ -hybrid parameters reflecting in the

experimental findings as follows: First of all, particularly  $S_{dr}$ —the percentage of the additional surface area contributed by the rough texture as compared to the ideal flat cross-section area—shows that the real area of contact considerably augments as the surface roughness decreases. The biggest change in  $S_{dr}$  by a factor of 22 was observed from #1000 to #2400, which accords well with the experimental findings and with the width of the breakdown channels shown in Figure 12. Second, the BD took place at the interface only three out of eight tests in the event of #2400 at 1.16 MPa. The rest occurred at the interface between the upper specimen and pressure transfer block (between upper no. 1 and no. 8 in Figure 6), and the corresponding data were regarded as the censored data in Figure 15. It was observed that the surface of the pressure transfer block being rough provided an easier path for the BD channel to propagate than the polymer interface did. Having polished that surface and having repeated the test; however, did not make a difference. Possibly, the BDS of the polymer interface was nearly as high as that of the bulk XLPE insulation ( $\approx 22 - 42$  kV/mm [17]); and hence, the BD took place at a weaker interface in the set-up (in the case of #2400 at 1.16 MPa). This finding supports that interfaces are the weaker parts of an electric insulation system.

**Table 2.** Surface roughness hybrid parameters.

Grit no.	$S_{ds}$ [ $1/\mu\text{m}^2$ ]	$S_{sc}$ [ $1/\mu\text{m}$ ]	$S_{dr}$ [%]
#180	0.02	2.633	1268.83
#500	0.04	1.318	665.21
#1000	0.04	0.924	44.51
#2400	0.04	0.096	2.12

Figure 18 features vertical error bars to represent the scatter of the 90% confidence intervals of the 63.2 percentile BDS as the surface roughness is varied. Seemingly, despite the increase in pressure, the overlap of the bars representing each pressure is significant in the case of the roughest surface (#180). Hence, voids of similar size are likely to arise irrespective of the pressure. On the other hand, the overlapping portions of the bars tend to decline as the surface smoothness increase. In the case of the smoothest surface, there is not any overlap as seen in Figure 18. Greenwood et al [18] addressed a related finding that the contact area augmented further as the contact pressure was increased, which yielded smaller voids at the interface.

Though a set of formulae or method is not proposed to estimate the expected interfacial BDS, the measured roughness parameters are found to be useful in interpreting the effect of surface texture on the interfacial BDS. The breakdown voltage of a single cavity is analogous to PD inception voltage as far as the interfacial discharge phenomenon is concerned [11]. The PD activity presumably commences at the largest cavity; however, how a few large cavities can form a channel and achieve a complete flashover along the interface was not directly studied. Nor was the duration until the PD activity evolves to a complete flashover examined. These unclear parts need to be further explored by including measurements of PD inception voltage/stress and by chasing after the largest cavities.

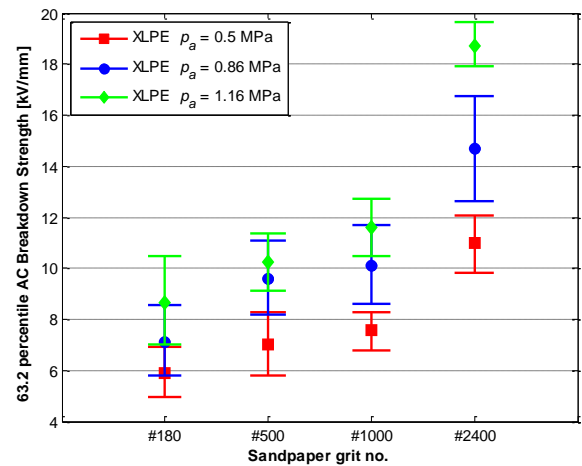


**Figure 18.** The 63.2 percentile BDS with 90% confidence intervals versus surface roughness represented by the mean roughness height parameter  $S_a$ .

## 6. CONCLUSION

The performed roughness measurements and the calculated  $S$ -height and -hybrid parameters e.g.  $S_a$  and  $S_{dr}$  correlated well with the experimental results. It was observed that the rougher the surface, the higher the peaks and valleys in the surface roughness profile. Thus, larger cavities are likely to form vented air-filled channels at the interface more easily, causing a lower BDS as discerned in the performed tests. It is noteworthy to have noticed that interfaces could perform as well as its intrinsic insulation does when the applied pressure is high enough, and the contact surface is as smooth as possible, as observed in the case of #2400 at 1.16 MPa. This conclusion translates into the fact that interfaces are weaker parts of an electric insulation system; however, it is possible to improve the performance of the polymer interface by introducing a smoother surface and by retaining the interfacial pressure high enough during service life.

## ACKNOWLEDGMENT

This work is funded by the project "High Voltage Subsea Connections (SUBCONN)." The project is supported by The Research Council of Norway (Project No. 228344/E30), and by the following industrial partners: ABB AS, Aker Solutions AS, Deutsch Offshore, Chevron Norge AS, Det Norske Oljeselskap ASA, Nexans Norway AS, Shell Technology Norway AS and Statoil Petroleum AS.

## REFERENCES

- [1] D. Fournier and L. Lamarre, "Effect of pressure and length on interfacial breakdown between two dielectric surfaces," IEEE Int'l. Sympos. Electr. Insul., pp. 270-272, 1992.
- [2] D. Kunze, B. Parmigiani, R. Schroth, and E. GocNenbach, "Macroscopic internal interfaces in high voltage cable accessories," CIGRE, 2000, pp. 15-203.
- [3] E. Kantar, D. Panagiotopoulos, and E. Ildstad, "Factors influencing the tangential AC breakdown strength of solid-solid interfaces," IEEE Trans. Dielectr. Electr. Insul., Vol. 23, No. 3, pp. 1778-1788, 2016.
- [4] M. Hasheminezhad and E. Ildstad, "Application of contact analysis on evaluation of breakdown strength and PD inception field strength of solid-solid interfaces," IEEE Trans. Dielectr. Electr. Insul., Vol. 19, pp. 1-7, 2012.

- [5] J. CIGRE, "21/15: Interfaces in accessories for extruded hv and ehv cables," *Electra*, No. 203, pp. 53-59, 2002.
- [6] T. Takahashi, T. Okamoto, Y. Ohki, and K. Shibata, "Breakdown strength at the interface between epoxy resin and silicone rubber—a basic study for the development of all solid insulation," *IEEE Trans. Dielectr. Electr. Insul.*, Vol. 12, pp. 719-724, 2005.
- [7] B. X. Du and L. Gu, "Effects of interfacial pressure on tracking failure between XLPE and silicon rubber," *IEEE Trans. Dielectr. Electr. Insul.*, Vol. 17, No. 6, pp. 1922-1930, 2010.
- [8] D. Fournier, C. Dang, and L. Paquin, "Interfacial breakdown in cable joints," *IEEE Int'l. Sympos. Electr. Insul.*, pp. 450-452, 1994.
- [9] D. Fournier and L. Lamarre, "Interfacial breakdown phenomena between two EPDM surfaces," *6th Int'l. Conf. Dielectr. Materials, Measurements and Applications*, pp. 330-333, 1992.
- [10] B. Du, X. Zhu, L. Gu, and H. Liu, "Effect of surface smoothness on tracking mechanism in XLPE-Si-rubber interfaces," *IEEE Trans. Dielectr. Electr. Insul.*, Vol. 18, No. 1, pp. 176-181, 2011.
- [11] L. A. Dissado and J. C. Fothergill, *Electrical Degradation and Breakdown in Polymers*, Vol. 9. IET, 1992.
- [12] A. Almqvist, "On the effects of surface roughness in lubrication," Ph.D. dissertation, Luleå tekniska universitet, pp. 31-37, 2006.
- [13] R. Leach, *Characterisation of areal surface texture*. Springer, pp. 15-44, 2013.
- [14] B. J. Jones, J. P. McHale, and S. V. Garimella, "The influence of surface roughness on nucleate pool boiling heat transfer," *J. Heat Transfer*, Vol. 131, No. 12, p. 121009, 2009.
- [15] "IEC/IEEE Guide for the Statistical Analysis of Electrical Insulation Breakdown Data (Adoption of IEEE Std 930-2004)," IEC 62539 First Edition 2007-07 IEEE 930, pp. 1-53, 2007.
- [16] K. C. Kao, *Dielectric Phenomena in Solids*. Academic press, pp. 530-532, 2004.
- [17] J. C. Chan, M. D. Hartley and L. J. Hiivala, "Performance characteristics of XLPE versus EPR as insulation for high voltage cables," *IEEE Electr. Insul. Mag.*, Vol. 9, No. 3, pp. 8-12, 1993.
- [18] J. Greenwood and J. Williamson, "Contact of nominally flat surfaces," *Proc. Royal Society of London A: Mathematical, physical and engineering sciences*, Vol. 295, pp. 300-319, 1966.



**Sverre Hvidsten** received the M.Sc. degree in 1992 at the Norwegian Institute of Technology (NTH) in Trondheim. During 1993 - 1994 he was a researcher at EFI in Norway. In 1999 he gained the Ph.D. in electrical engineering at The Norwegian University of Science and Technology, NTNU in Trondheim. He then joined SINTEF Energy Research (SEfAS). He is now Research Manager for the Electrical Insulation Material group at SEfAS. He also participates in CIGRE work.



**Emre Kantar** (M'14) received the B.Sc. and M.Sc. degrees in electrical engineering from Middle East Technical University, Ankara, Turkey, in 2011 and 2014, respectively. From 2010 to 2014, he was with ASELSAN, Inc., Ankara and worked as an R&D engineer. He is currently a Ph.D. candidate at the Department of Electric Power Engineering, Norwegian University of Science and Technology, in Trondheim, Norway. His research interests include dielectric breakdown in solids, high voltage

equipment and insulation materials, and power electronics.



**Frank Mauseth** (M'11) received his M.Sc. degree in electrical engineering from Delft University of Technology, The Netherlands, in 2001. Since then he has been with the Norwegian University of Science and Technology (NTNU) in Trondheim, Norway, where he also received his Ph.D. degree in 2007 and now is working as an Associate Professor at NTNU. Main fields of interest are high voltage insulation materials and systems, measurement methods and testing. He is active in the IEEE DEIS

TC "HVDC Cable Systems" and CIGRE WG D1.48.



**Erling Ildstad** received the M.Sc. degree in technical physics in 1978 and the Ph.D. degree in electrical power engineering in 1982 from the Norwegian University of Science and Technology (NTNU) in Trondheim, Norway. Since then his main research activity has been related to the development and testing of insulation systems for ac and dc power cables. He has been a full-time professor of high voltage engineering at NTNU

since 1993 and has been the head of the Electric Power Engineering Department from 1998 to 2008 and 2011 onward.